

Vacuum Microelectronics and Miniature Instruments Based on Application Specific electrode-Integrated Nanotube Cathodes (ASINCs)

H.M. Manohara, M.J. Bronikowski, R. Toda, E. Urgiles, K.Y. Yee, A.B. Kaul, and M.M. Mojarradi

Jet Propulsion Laboratory
California Institute of Technology
Pasadena, California, USA, Zip: 91109

Abstract: JPL has developed high performance cold cathodes using arrays of carbon nanotube bundles that routinely produce $> 15 \text{ A/cm}^2$ at 5 to 8 $\text{V}/\mu\text{m}$ applied fields for extreme environment vacuum electronics and miniature instrumentation. These cathodes have been monolithically integrated with additional electrodes using double silicon-on-insulator process. The cathodes have been found to operate well in individually packaged vacuum cavities using commercial off-the-shelf parts even after 6 months of shelf-life. Radiation-insensitive vacuum digital electronics, miniature X-ray tubes for future mineralogy instruments, and high-performance ionization sources for miniature mass spectrometers are being developed.

Keywords: Field Emission; Carbon Nanotube; CNTs; Vacuum; Microelectronics

Introduction

Background: Micro and nanotechnology development activities at JPL are directed toward enhancing the data-collection capabilities and overall science return on NASA missions to planets and planetary bodies without significantly increasing the payload. Efficient electron sources are the fundamental components of- (i) multiple analytical instruments to perform elemental and mineralogical analyses [1], (ii) vacuum microelectronic devices to develop radiation-insensitive, extreme environment withstanding electronics, and (iii) miniature vacuum tube sources for high frequency applications [2]. Each application requires specifically designed electron source in terms of beam forming optics and the emission density that spans a range of tens to hundreds of amperes per sq. cm. The state-of-the art thermionic cathodes are ill-suited for miniature instruments because of their bulkiness, high temperature operation, and high power consumption. The state-of-the-art cold cathodes [3] that are based on atomically sharp micromachined tips [4,5] are highly susceptible to poisoning when operated in non-UHV (10^{-8} to 10^{-9} Torr) environments. Such vacuum levels are not possible to attain in micromachined vacuum cavities necessary for miniaturization.

Carbon Nanotube Field Emitters: A new class of field emitters was identified when carbon nanotubes (CNTs) were discovered [6]. CNTs offer sharp tips that are one to several tens of nanometer in diameter. A single tip is known to produce tens of nA of current at very low

threshold fields, less than 1 $\text{V}/\mu\text{m}$ [7]. Additionally what makes them attractive is their robustness to poor vacuums. They operate well in low vacuum ranges of 10^{-4} to 10^{-5} Torr, which is typically what one can achieve using the standard micromachining processes. However, it was found that the high current emission ability of single, isolated tip does not scale up when multiple tips are employed simultaneously due to the *electrostatic screening effect* [8] or “hot spots”. With multiple tips, only those CNTs with locally the highest field enhancement factor (or β -factor) participate in electron emission. Many research groups have reported different optimum CNT arrangement [8-12], to minimize these *hot spots*, and achieve high, uniform emission currents. But producing tens to hundreds of A/cm^2 on a routine basis is still an active area of research. At JPL, we have been able to achieve tens of A/cm^2 at low fields by employing array architecture of CNT bundles with specific diameter and spacing.

Application Specific electrode-Integrated Nanotube Cathodes (ASINCs)

Carbon Nanotube Bundle Arrays: In our pursuit of high-performance field emitters, we have found that CNTs when arranged as arrays of 1-2 micrometer (μm) diameter bundles spaced 5 μm apart (see Figure 1) give very high emission current densities [13]. After initially achieving $> 2 \text{ A/cm}^2$ at 4 $\text{V}/\mu\text{m}$, we have optimized the CNT growth

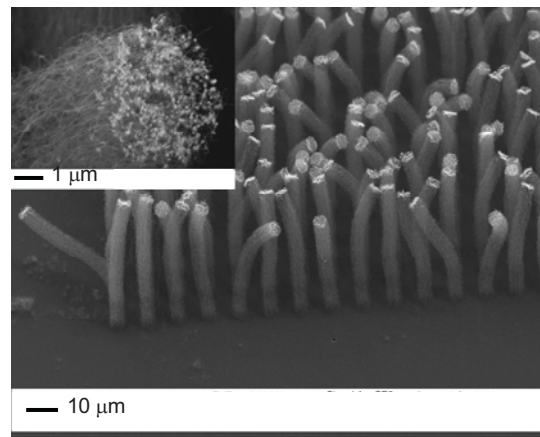
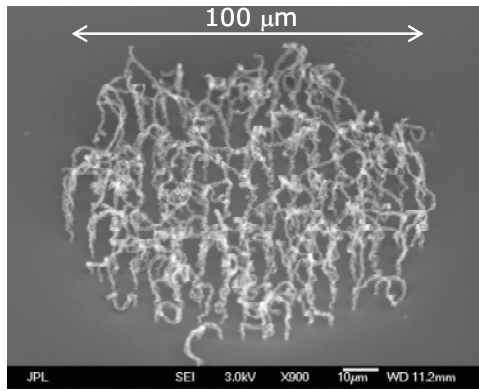
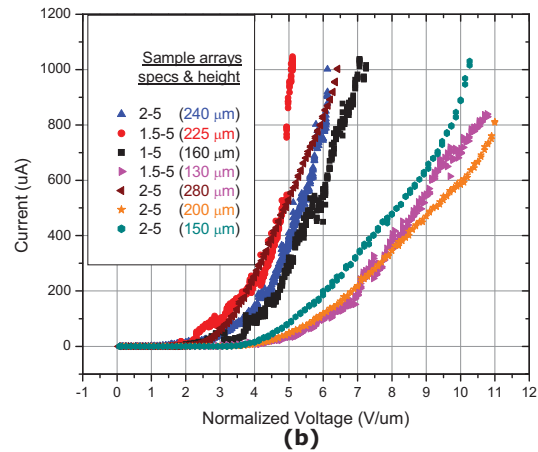


Figure 1. SEM micrograph of optimum CNT bundle arrays (1 μm diameter spaced 5 μm edge-to-edge). Inset shows the magnified view of one of the bundles containing hundreds of 20 nm-diameter nanotubes.



(a)



(b)

Figure 2. (a) SEM micrograph of 100- μm diameter sample with 1- μm diameter bundles. (b) An example of field emission data from multiple samples producing 10 to 15 A/cm^2 at fields ranging from 4 to 9 $\text{V}/\mu\text{m}$.

process and the architecture in recent times to routinely produce 10 to 25 A/cm^2 at applied fields of 5 to 10 $\text{V}/\mu\text{m}$ [14]. These tests were conducted using CNT bundle array samples that occupied a circular area of 100 μm diameter (see Figure 2(a)), which is considered a large area source for our applications. The repeatability of this current production was achieved over multiple samples as shown in Figure 2(b). All emission tests were conducted in $\sim 10^{-5}$ Torr vacuum.

The reason for high emission from bundle arrays is not yet clearly understood, however, real time SEM observation has revealed that *free-ends* and *outliers* in each bundle rearrange themselves under an applied field [15] causing high field enhancements (γ -factor), which may be resulting in efficient field emission. Typically we have measured γ -factor values of 2,000 to 8,000 from CNT bundle array samples, which are high compared to other field emitters. In large area sources, the initial emission occurs from the highest γ -factors tubes (which accounts for the low threshold fields: 1-3 $\text{V}/\mu\text{m}$) followed by from those CNTs with lower γ -factors as the applied field is increased. Because of the latter effect, the average γ -factor of the entire sample decreases at higher fields, somewhat flattening the higher field part of the Fowler-Nordheim curve [16] (see Figure 3).

Using a theoretical relation, Bonard *et al* [17] have shown that for an isolated nanotube, the γ -factor increases as a function of its aspect ratio before approaching a plateau. Similar behavior was observed for large area CNT bundle array samples as well. Measured γ -factors for different bundle diameters as a function of bundle height are shown in Figure 4. For a given diameter bundle array, the γ -factor (and consequently the emitted current) increases towards saturation as the height of the bundles is increased (data is shown up to a bundle height beyond which, the weight of the bundles overcomes their stiffness to conduct accurate measurements). For the applications discussed here,

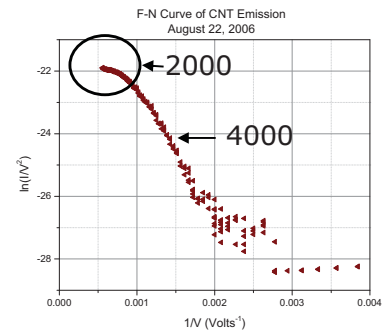


Figure 3. Experimental demonstration of the averaging effect of field enhancement factor (γ -factor) for a large area sample, which has a flattening effect on the Fowler-Nordheim curve at higher fields. In this example, the average γ decreases from 4000 to 2000 at higher fields.

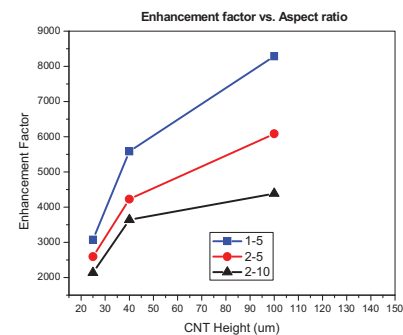


Figure 4. Experimental verification of the variation of the γ -factor as a function of CNT-bundle height. As the aspect ratio increases the γ -factor approaches saturation.

typically 8 to 20 μm tall bundles were used for electron sources.

Vacuum Packaged CNT Bundles: Field emission performance of CNT bundles inside a stand-alone vacuum package has been tested using an optimized solder-reflow process [18]. CNT chips were mounted inside COTS packages (LCC packages) and were closed off using getter (proprietary composition) patterned Kovar metal discs. The bonding was performed using Au/Sn solder reflow process at 290° C. Prior to bonding, samples were pre-baked for 96 hours and the bonding itself was conducted at 10^{-7} Torr vacuum. Figure 5-inset shows a vacuum packaged CNT chip. These samples were field emission tested for vacuum integrity after six months of shelf life (curve shown in Figure 5). The measured current corresponds to a vacuum of 10^{-6} to 10^{-5} Torr, indicating the robustness of the process. We are employing this process to produce vacuum digital electronics.

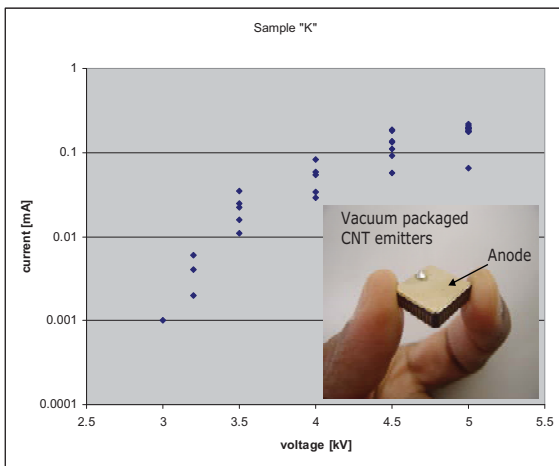


Figure 5. A field emission curve that was measured by biasing a vacuum packaged CNT chip. Inset: Vacuum packaged CNT using LCC-package and solder reflow bonding technique.

Monolithic Electrode Integration: Miniature instruments and vacuum electronics applications require electron beam

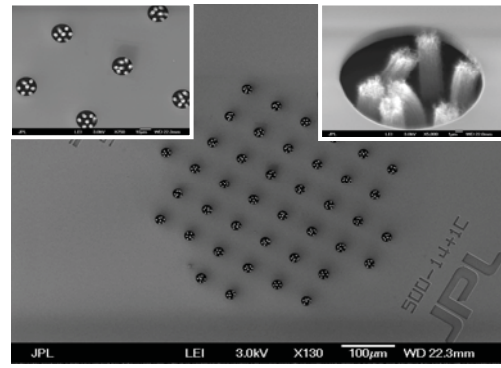


Figure 6. SEM micrograph of monolithically gate-integrated CNT bundle cathode using double-SOI structure. The two insets show different magnification of a cell.

tailoring. This is achieved by adding extraction, focusing, and acceleration electrodes. Using double SOI substrates we have developed a process to monolithically integrate electrodes with CNT bundles [19]. A combination of lithography, wet and deep-reactive ion etching are used to create a well in the substrate down to the thick bulk silicon layer. Iron catalyst dots are patterned at the bottom of the well followed by CNT growth in the patterned areas using a CVD process. Because CNT bundles are free to move under applied fields, a thermal oxide layer is formed to cover electrodes to prevent shorting. Figure 6 shows a multi-bundle gate-integrated structure. The double SOI process allows flexibility to integrate multiple levels of electrodes, if required, via stacking.

Lifetime Issues: We have found that, when operated in a continuous mode, the performance of ASINCs is affected by two effects- (i) a gradual decay of emission due to anode sputtering at lower fields (< 10 V/ μ m), and dislodging of CNT bundles from the substrates at higher fields (> 10 V/ μ m). The former effect has been observed in traditional cold cathodes [20]. But, the latter is unique to CNT field emitters. Figure 7(a) shows a gradual decay of field

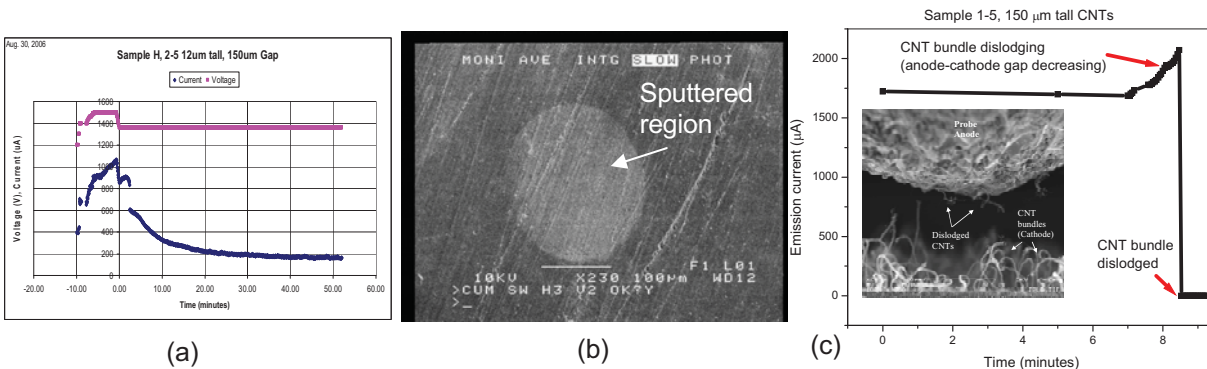


Figure 7. (a) Graph showing a gradual decay of field emission current in continuous bias mode. Top curve indicates bias voltage (held constant after $t=0$); (b) SEM micrograph of glassy carbon anode showing etched circular region corresponding to CNT cathode area; (c) Graph showing the high field failure of field emission due to CNTs dislodging from the surface. The inset shows SEM micrograph of dislodged CNTs stuck to the probe

emitted current from > 1 mA to ~ 200 μ A within 20 minutes. Over several samples we have observed that the emission current eventually settles down to around 200 μ A. These experiments were conducted using copper and glassy carbon anodes. EDX analysis of a CNT sample tested using Cu showed sputtered copper particles settled on CNTs. Similarly, SEM micrograph of glassy carbon anode showed a circular etched region (see Figure 7(b)) corresponding in dimension and location to the cathode.

When the field is increased to > 10 V/ μ m, we start seeing the second failure mechanism. The force exerted at these fields seems large enough to dislodge individual CNT bundles (presently measured adhesion strength of CNT bundles to the Si substrate is ~ 35 to 65 kPa). This is shown in Figure 7(c). The graph shows a continuously increasing emission current even though the bias voltage is kept constant, indicating slowly rising CNT bundle(s) that have been dislodged but are held down by surrounding bundles. A sharp drop in the emission current indicates the bundle(s) completely losing any contact with the cathode. The inset of Figure 7(c) shows SEM micrograph of an anode tip that has dislodged CNT bundles attached to it. We are currently developing techniques to mitigate both of the effects mentioned above. Initial tests have shown continuous high field operation for tens of hours.

This research was carried out at the Jet Propulsion Laboratory, California Institute of Technology, under a contract with National Aeronautics and Space Administration (NASA). This work was funded by JPL's Research and Technology Development Fund and by Defense Advanced Research Project Agency seedling fund (Task Order NMO#715839 under NAS7-03001).

References

1. D. Vaniman, D. Bish, D.F. Blake, S.T. Elliot, P. Sarrazin, S.A. Collins, S. Chipera, *J. Geophys. Res.*, 103(E13), pp. 31,477-31,489 (1998).
2. P.H. Siegel, A. Fung, H.M. Manohara, J. Xu, B. Chang, "Nanoklystron: A Monolithic Tube Approach to THz Power Generation," *Proc. 12th International Symposium on Space Terahertz Technology*, pp. 94-103 (2001).
3. R. Gomer, "Field Emission and Field Ionization," AVS Classics Series, American Institute of Physics, New York (1993).
4. C.A. Spindt, I. Brodie, L. Humphrey, E.R. Westerberg, "Physical properties of thin-film field emission cathodes with molybdenum cones," *J. Appl. Phys.*, Vol. 47 (12), pp. 5248-5263 (1976)
5. J.T. Trujillo, C.E. Hunt, "Fabrication of gated silicon field-emission cathodes for vacuum microelectronics and electron-beam applications," *J. Vac. Sci. Technol. B*, Vol. 11(2), pp.454-458 (1993).
6. S. Ijima, "Helical microtubules of graphitic carbon," *Nature*, Vol. 354, pp. 56-58 (1991).
7. J.M. Bonard, H. Kind, T. Stöckli, L. Nilsson, "Field emission from carbon nanotubes: the first five years," *Solid-State Electron.*, Vol. 45, pp. 893-914 (2001).
8. L. Nilsson *et al*, "Scanning field emission from patterned carbon nanotube films," *Appl. Phys. Lett.*, vol. 76, pp. 2071-2073 (2000).
9. H. Murakami, H.; Hirakawa, M.; Tanaka, C.; Yamakawa, H. "Field emission from well-aligned, patterned, carbon nanotube emitters," *Appl. Phys. Lett.*, Vol. 76, pp. 1776-1778 (2000).
10. W. Zhu, C. Bower, G.P. Kochanski, S. Jin, "Electron field emission from nanostructured diamond and carbon nanotubes," *Solid-State Electron.*, Vol. 45, pp. 921-928 (2001).
11. J.S. Suh, K.S. Jeong, J.S. Lee, I. Han, "Study of field screening effect of highly ordered carbon nanotube arrays," *Appl. Phys. Lett*, Vol. 80, pp. 2392-2394 (2002).
12. K.B.K. Teo *et al*, "Field emission from dense, sparse, and patterned arrays of carbon nanofibers," *Appl. Phys. Lett.*, Vol. 80, pp. 2011-2013 (2002).
13. H.M. Manohara, M.J. Bronikowski, M. Hoenk, B.D. Hunt, P.H. Siegel, "High-current-density field emitters based on arrays of carbon nanotube bundles," *Journal of Vacuum Science and Technology B*, Vol. 23(1), 157-161 (2005).
14. H. Manohara, *et al*, "Application Specific electrode-Integrated Nanotube Cathodes (ASINCs) for Miniature Analytical Instruments for Space Exploration," To appear in the *Proceedings of SPIE Defense and Securities Symposium*, Orlando, FL, March 2008.
15. H.M. Manohara *et al*, "Carbon nanotube bundle-based cold cathodes for THz tube sources," *International Conference on Infrared, Millimeter Wave Technologies*, Williamsburg, VA, September 2005.
16. R.H. Fowler, L.W. Nordheim, *Proc. R. Soc. London*, Ser. A 119, pp. 173 (1928).
17. J.M. Bonard, K.A. Dean, B.F. Coll, and C. Klinke, "Field emission of individual carbon nanotubes in the scanning electron microscope," *Phys. Rev. Lett.*, Vol. 89 (19), pp. 197602-1-4 (2002).
18. *Private communications* with Dr. Karl Yee, Jet Propulsion Laboratory.
19. R. Toda, M.J. Bronikowski, E. Luong, H. Manohara, "New double-SOI process to fabricate gated high-performance CNT cathode," *JPL New technology Reports*, NPO 44996, April 2007.
20. *Private communications* with Dr. Dev Palmer, US Army Research Office.